Received: 8 June 2022 | Revised: 29 October 2022 | Accepted: 30 December 2022

DOI: 10.1111/ter.12643

RESEARCH ARTICLE

Terra Nova WILEY

# Accretionary orogenesis triggered by collision across continent distance: Evidence from the Proto-Tethyan West Kunlun, China

Yan-Jun Wang[1,2] | Wei-Guang Zhu[2] | Zheng-Wei Zhang[2] | Kang Yang[2] | Cheng-Quan Wu[2] | Jin-Hong Xu[2,3] | Cheng-Biao Leng[1] | Jian-Bing Xu[1]

[1]State Key Laboratory of Nuclear Resources and Environment, East China University of Technology, Nanchang, China

[2]State Key Laboratory of Ore Deposit Geochemistry, Institute of Geochemistry, Chinese Academy of Sciences, Guiyang, China

[3]School of Economics and Management, Tongren University, Tongren, China

**Correspondence**
Wei-Guang Zhu, State Key Laboratory of Ore Deposit Geochemistry, Institute of Geochemistry, Chinese Academy of Sciences, 99 West Lincheng Road, Guiyang 550081, China.
Email: zhuweiguang@vip.gyig.ac.cn

**Funding information**
National Natural Science Foundation of China, Grant/Award Number: 42002210 and U1603245; State Key Laboratory of Ore Deposit Geochemistry, Institute of Geochemistry, Chinese Academy of Sciences, Grant/Award Number: 202212

## Abstract

Proto-Tethyan orogenic processes prior to the late Ordovician collision remain unclear. Both whole-rock La/Yb- and zircon Eu/Eu*-based crustal thickness proxies along with petrological and geological observations were used to reconstruct mountain-building history for the West Kunlun orogenic belt, China, over the span of Early Palaeozoic. Here, we demonstrate that Proto-Tethyan West Kunlun crust has observed significant accretionary orogeneses at 520–480 Ma and 480–450 Ma and collisional orogenesis at 450–400 Ma. The 520–480 Ma accretionary orogenesis in West Kunlun together with the coeval Delamerian accretionary contractional orogenesis in eastern Australia were simultaneously induced by continent-continent collisions that welded the Gondwana landmass. Ca. 440 Ma docking of Tarim and its eastern neighbouring blocks along the northern margin of Gondwana in turn triggered the Lachlan accretionary orogenesis along the opposite margin. This study highlights that accretionary orogenesis could be a manifestation of far-field compressional stress from continent-continent collision.

## 1 | INTRODUCTION

A classic, intact Wilson cycle predicts mountain-building processes at the very end of the cycle marked by continent-continent collision (Cawood et al., 2009). Modern example for this is the Alpine-Himalayan mountain chain raised by the collision between Eurasian and African-Indian plates. Another type of mountain-building is the accretionary orogenesis that occurs during continuing subduction and accretion as represented by accretionary orogens along the western and northern Pacific (Cawood et al., 2009). Accretionary orogens could be induced by the accretion of the buoyant lithosphere, flat-slab subduction and rapid absolute upper plate motion overriding the downgoing plate (Cawood et al., 2009). How accretionary and collisional orogeneses interact is less known because they preferentially occur at different stages of the Wilson cycle of an oceanic basin. We investigated this issue by comparing mountain-building processes in Proto-Tethyan West Kunlun with those in neighbouring Gondwana.

The Proto-Tethys Ocean was an Early Palaeozoic ocean that developed between two linearly-distributed groups of Asian (micro-) continental blocks, including the Greater South China-North China-Alax-Dunhuang-Tarim blocks to the north and the North Qinling-Central Qinling-Central Altyn-East Kunlun (NQ-CQ-CA-EK) terranes to the south (He et al., 2016; Li et al., 2016, 2018). Its final closure led to the docking of the Greater South China-North China-Alax-Dunhuang-Tarim blocks along the northern margin of Gondwana (containing the NQ-CQ-CA-EK terranes; Figure 1; Li et al., 2018). The collision process was well documented by the ~450 Ma high- to ultrahigh-pressure metamorphism (e.g. Li et al., 2018; Zhang et al., 2017; Zhou et al., 2000). However, Proto-Tethyan orogenic processes prior to the late Ordovician collision are not studied in sufficient detail.

  

Continents tend to have an elevation close to sea level due to the balance of erosion and deposition (Rowley, 2013). However, active continental margins commonly obtain remarkably huge thicknesses due to tectonic compression and magmatic inflation during mountain-building processes. Orogenic crust quickly loses its thickness due to enhanced erosion and gravitational collapse (Tang et al., 2021). Mountains are thereby ephemeral. The recently calibrated crustal thickness proxies (e.g. whole-rock La/Yb and zircon Eu/Eu*) allow to reconstruct mountain-building history of ancient orogens (Profeta et al., 2015; Tang et al., 2020).

Here, we recovered crustal thickness variations of the West Kunlun orogenic belt, China, during the whole life of Proto-Tethys Ocean using crustal thickness proxies. Proto-Tethyan accretionary and collisional orogeneses have been identified in West Kunlun and were further compared with other Early Palaeozoic orogeneses within and along the eastern margin of Gondwana to decipher Proto-Tethyan dynamic processes.

**Statement of Significance**

The West Kunlun orogenic belt preserves intact geological records of Proto-Tethyan subduction and collision. Here, we present a perspective of crustal thickness variation to identify mountain-building processes in Proto-Tethyan West Kunlun. Newly recognized accretionary orogenesis (e.g. 520–480 Ma) in West Kunlun, together with those in eastern Australia (the Delamerian and Lachlan Orogens) have been proposed to be triggered by continent-continent collisional events across continent distance. This study exemplifies a case of an alternative geological response to collision rather than an induced subduction initiation, which depends on whether there is existing subduction or not.

## 2 | GEOLOGICAL SETTING

The West Kunlun orogenic belt occupies a NW–SE-striking, narrow zone between the Tarim Block and the Tibetan Plateau (Figure 2a). It contains the North Kunlun Terrane (NKT), the South Kunlun Terrane (SKT) and the Tianshuihai Terrane (TSHT) from north to south, which are separated by the Kudi-Qimanyute suture and the Mazha-Kangxiwa suture, respectively (Figure 2b). The NKT has a Paleoproterozoic basement and represents the southern margin of the Tarim Block. The SKT was previously thought to be drifted from Tarim (Matte et al., 1996), but a recent investigation argues against the existence of a basement older than late Neoproterozoic for the SKT (Zhang, Zou, et al., 2019). The TSHT has the late Neoproterozoic Tianshuihai Group as basement (Zhang, Zou, et al., 2019).

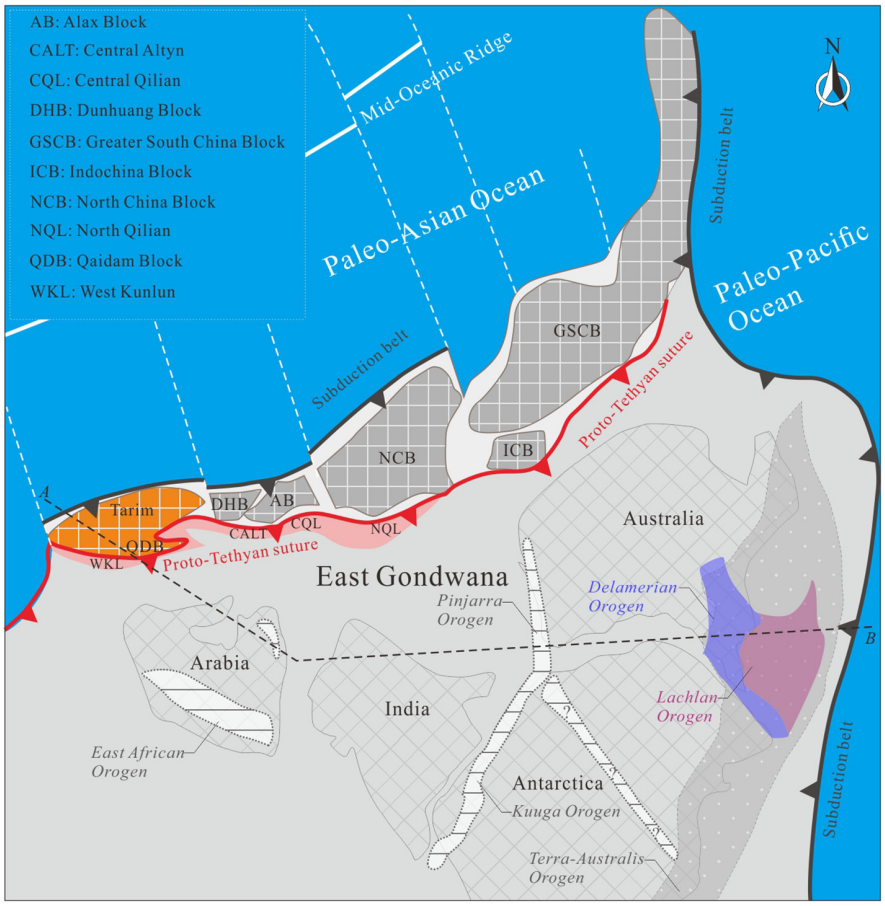


FIGURE 1 Reconstruction of East Gondwana at 430 Ma (modified after Li et al., 2018). The 520–490 Ma Delamerian accretionary Orogen and 440–400 Ma Lachlan accretionary Orogen in the eastern margin of Australia Block (Collins et al., 2019) are specially outlined. Both the Delamerian Orogen and Lachlan Orogen are important parts of the Neoproterozoic to late Palaeozoic Terra Australis Orogen, which extended along the eastern-southern margin of Gondwana (approximately 18 000 km; Cawood, 2005). The Pinjarra Orogen, Kuuga Orogen and East African Orogen within Gondwana are also shown for comparison. Note that the West Kunlun orogenic belt along the northern margin of Gondwana has experienced Early Palaeozoic southward subduction of Proto-Tethys Ocean, contrasting with the long-lived westward subduction of Paleo-Pacific Ocean beneath eastern Australia in the eastern margin of Gondwana. [Colour figure can be viewed at wileyonlinelibrary.com]

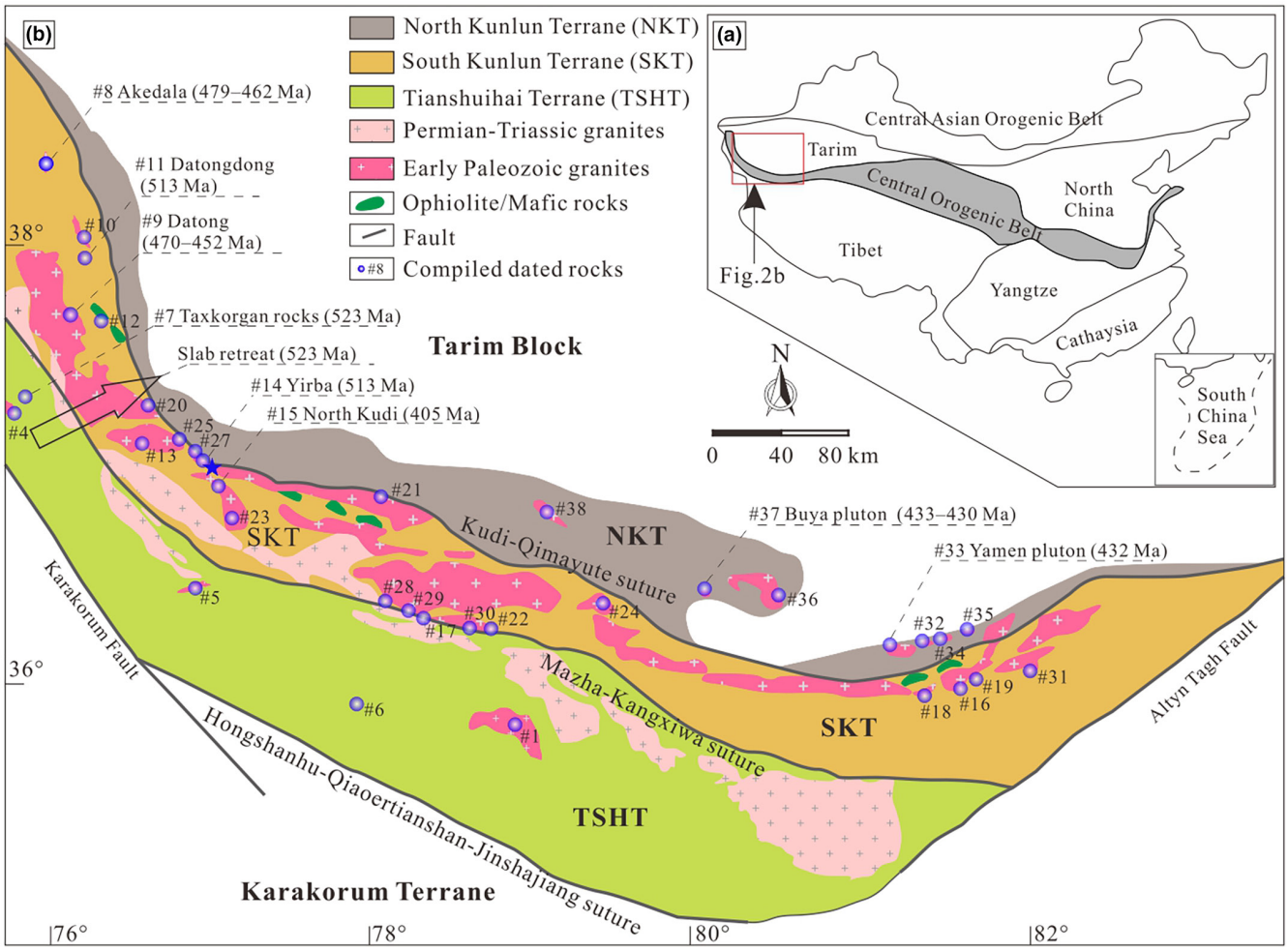


FIGURE 2 A sketch map of China (a) and a geological map of the West Kunlun orogenic belt (b; modified after Zhang, Wu, Chen, et al., 2019). Most of compiled dated Early Palaeozoic magmatic rocks are shown. Key magmatic rocks are specially marked. These rocks were compiled from (Cui et al., 2006; Cui, Wang, Bian, Zhu, et al., 2007; Cui, Wang, Bian, Luo, et al., 2007; Gao et al., 2013; Hu, 2018; Hu et al., 2016; Hu, Wang, et al., 2017; Hu, Guo, et al., 2017; Jia et al., 2013; Li et al., 2019; Liao et al., 2010; Liu et al., 2014, 2016, 2019; Wang et al., 2013, 2017; Xiao et al., 2005; Xu et al., 2021; Ye et al., 2008; Yin et al., 2020; Yuan et al., 2002; Zhang et al., 2007; Zhang, He, et al., 2016; Zhang, Liu, et al., 2016; Zhang et al., 2018a; Zhang, Wu, Chen, et al., 2019; Zhang, Wu, Li, et al., 2019; Zheng et al., 2013; Zhu et al., 2016, 2018; Zhuan et al., 2018). Please see Table S2 for more details. In addition, blue star represents the location of detrital zircons (Zhang et al., 2022) used for crustal thickness calculation. Slab retreating event is according to Yin et al. (2020). [Colour figure can be viewed at wileyonlinelibrary.com]

The Proto-Tethys Ocean was proposed to be located either between SKT and TSHT with a north-dipping subduction polarity (e.g. Hu, Wang, et al., 2017; Yin & Harrison, 2000) or between NKT and SKT with a south-dipping subduction polarity (current orientation; e.g. Yin et al., 2020; Zhang et al., 2018a, 2018b; Zhang, Zou, et al., 2019). The supra-subduction zone-type nature of the ~510 ± 4 Ma Kudi ophiolite suite (Xiao et al., 2003; Yuan et al., 2005) along the Kudi-Qimanyute suture is consistent with the latter model. Recently identified ~530 Ma metasomatized asthenospheric mantle-derived gabbros (Zhang et al., 2018a) and coeval I-type granites (Yin et al., 2020) in the northern margin of TSHT not only provide additional arguments for the southward subduction polarity but also suggest that the subduction of the Proto-Tethys oceanic plate should have initiated somewhat earlier than 533 Ma. Subduction of the Proto-Tethys oceanic plate continued till 450 Ma (Zhang, Zou, et al., 2019).

## 3 | METHODS AND RESULTS

### 3.1 | Methods

This study used whole-rock La/Yb (Profeta et al., 2015) and zircon Eu/Eu* (Tang et al., 2020) methods to quantitatively recover the crustal thickness of West Kunlun in Early Palaeozoic. Other methods have been discarded for reasons listed in Supporting Materials.

We compiled available published zircon U-Pb ages and whole-rock major-trace element data of Early Palaeozoic magmatic rocks in the West Kunlun orogenic belt. A dataset was collected from over 37 locations (plutons) with 78 mean zircon U-Pb ages (Table S2). The dataset was filtered following rules in Supporting Materials. The filtered data (Figure 3) were used for crustal thickness calculation following equation (1) $d_m = 21.277 \times \mathrm{Ln}(1.0204 \times [\mathrm{La/Yb}]_N)$ (N represents chondrite normalization; Profeta et al., 2015).

Magmatic zircon grains were extracted from three granite samples (AKDL-2, AKDL-4 and AKDL-8) of the Akedala pluton for in situ trace elements analysis along with U-Pb dating. Analytical conditions and data reduction processes were described in Xu et al. (2021), which also reported accompanying zircon U-Pb data. Crustal thickness based on zircon Eu/Eu* was calculated according to equation (2) $d_m = (84.2 \pm 9.2) \times [Eu/Eu^*]_{zircon} + (24.5 \pm 3.3)$ (2 sigma; Tang et al., 2020), where $d_m$ is the crustal thickness in km. The I-type nature of the Akedala pluton (Xu et al., 2021) guarantees the applicability of the equation.

We compiled trace elements and accompanying ages of detrital zircons from a single location in Proto-Tethyan West Kunlun (Zhang et al., 2022). The data were filtered to have P < 750 ppm and La < 1 ppm to preclude potential effects from S-type rocks and inclusions. Only detrital zircons younger than 540 Ma with concordance better than 94% were used for crustal thickness calculation following equation (2).

### 3.2 | Results

Filtered, compiled whole-rock La/Yb ratios yield crustal thicknesses of 31.6 to 104 km (Figure 4).

Magmatic zircon trace element data were listed in Table S1 and evaluated in Supporting Materials. Eu/Eu* values of AKDL-2, AKDL-4 and AKDL-8 correspond to the crustal thickness of 44.1–50.0, 37.5–43.9 and 62.6–83.8 km, respectively (Figure 4).

Filtered, compiled detrital zircons have Eu/Eu*-based crustal thickness of 33.5–90.1 km (Figure 4).

## 4 | DISCUSSION

### 4.1 | Variations of crustal thickness over time

Because equations (1) and (2) were calibrated for crust thickness between 10 to 70 km (Profeta et al., 2015; Tang et al., 2020), crustal thickness estimates in this study are thereby reliable for most of the data except for those over 70 km. Nonetheless, it is still convincing that the Proto-Tethyan West Kunkun has attained an over 70 km crustal thickness at 430 Ma given the overall elevated La/Yb ratios for ~430 Ma rocks.

Proto-Tethyan West Kunlun shows evidently cyclical changes in crustal thickness over time (Cycle I–IV; Figure 4). Proto-Tethyan West Kunlun had a crustal thickness of ~54.5 km at 530 Ma, which declined to a normal continental crustal thickness (~38.6 km) at 520 Ma (Cycle I). Cycle I thinning event is consistent with the presence of ~523 Ma Taxkorgan bimodal volcanic rocks in an extensional setting (Gao et al., 2013) and the northward migration of arc magmatism from TSHT to SKT at the duration (Yin et al., 2020). An intact crustal thickening and thinning process occurred from 520 Ma to 480 Ma

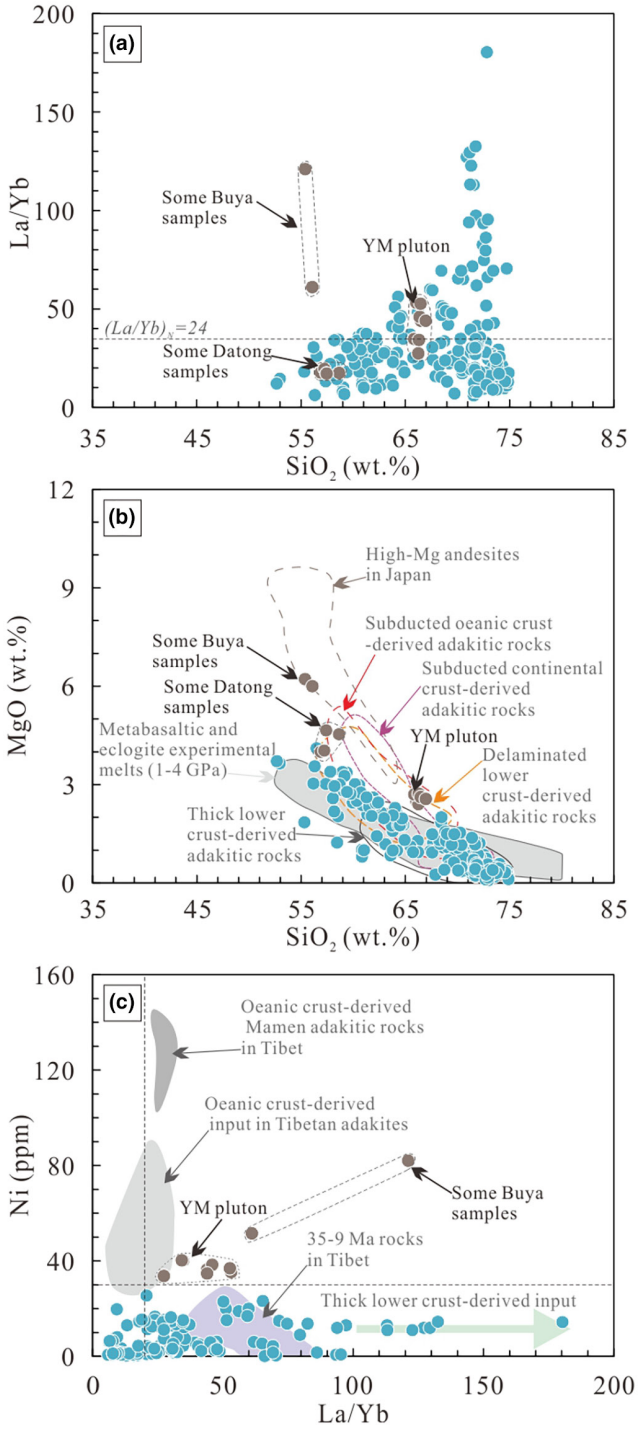


FIGURE 3 Diagrams of (a) $SiO_2$ vs. La/Yb, (b) $SiO_2$ vs. MgO and (c) La/Yb vs. Ni for complied Early Palaeozoic magmatic rocks after filtering. Brown dots represent some unique samples that were produced by melts from either subducted oceanic/continental crust or delaminated lower crust, including several Buya samples, several Datong samples and all Yamen (YM) samples. However, note that most of the Buya and Datong samples are originated from a thick lower crust. Data sources of Early Palaeozoic magmatic rocks as Figure 2. Reference fields in a are from Tang et al. (2010) and references therein; Tibetan rocks in b are from Zhu et al. (2017). [Colour figure can be viewed at wileyonlinelibrary.com]

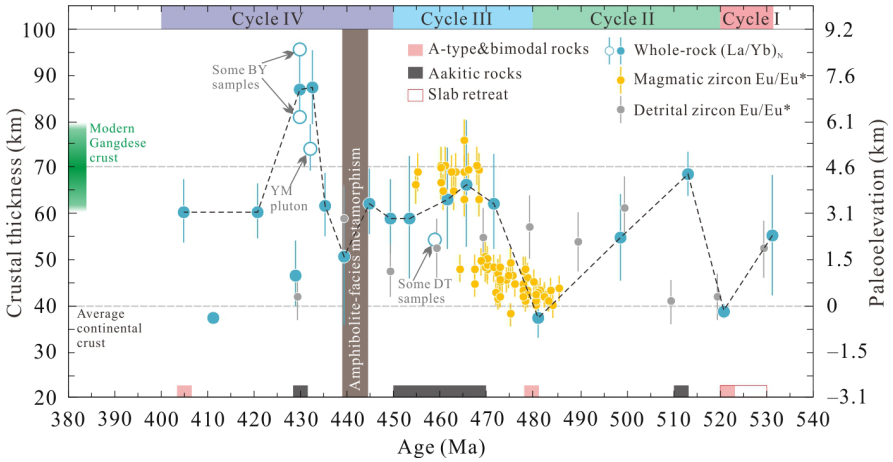


**FIGURE 4** Reconstructed history of crustal thickness and paleoelevation changes for Proto-Tethyan West Kunlun. La/Yb-based crustal thickness estimates show episodic crustal thickening and thinning processes, which were divided into four cycles (I to IV). These crustal thickening and thinning events are supported by accompanying geological evidences including A-type or bimodal rocks (~523 Ma Taxkorgan rocks, ~478 Ma Kusilafu pluton and ~405 Ma North Kudi pluton; Gao et al., 2013; Li et al., 2019; Xiao et al., 2005; Yuan et al., 2002), adakitic rocks (~513 Ma Datongdong and Yirba plutons, 470–452 Ma Datong and Akedala plutons and 430 Ma Buya pluton; Hu, Guo, et al., 2017; Li et al., 2019; Liao et al., 2010; Liu et al., 2014; Wang et al., 2017; Xu et al., 2021; Ye et al., 2008; Yin et al., 2020; Zhu et al., 2018), ~520 Ma northward migration of arc magmatism (Yin et al., 2020) and ~440 Ma amphibolite-facies metamorphism (Zhang, Zou, et al., 2019). Crustal thickness estimates from magmatic zircons are in agreement with those from the whole-rock La/Yb method. Detrital zircons from a single location in West Kunlun (Zhang et al., 2022) also give broadly consistent results. Binned median values with 1 sigma error (bin size, 10 Myr) were plotted for calculated results from detrital zircons and whole-rock La/Yb ratios; data from magmatic zircons were directly plotted without median calculation. Note unique samples (some Buya (BY) samples, some Datong (DT) samples and all of Yamen (YM) samples) were specially marked (hollow green circles) due to their geochemical features of subducted oceanic crust- or delaminated lower crust-derived adakitic rocks (high MgO and Ni contents; Figure 3b,c). Paleoelevation was calculated assuming Airy isostatic compensation following equation (3) $d_p = (d_m - d_{nm})/[(\rho_{lm}/(\rho_{lm}-\rho_c)]$, where $d_p$, $d_m$ and $d_{nm}$ are paleoelevation, previously calculated crustal thickness and normal crustal thickness (~40 km; Rudnick & Gao, 2003) in km, respectively; $\rho_c$ and $\rho_{lm}$ are the crustal density of 2.77 g/cm$^3$ and lithospheric mantle density 3.27 g/cm$^3$, respectively (He et al., 2014). Thickness of modern Gangdese crust (60–80 km; Tang et al., 2020) is shown for comparison. [Colour figure can be viewed at wileyonlinelibrary.com]

with a maximum thickness of ~68.1 km (510 Ma) (Cycle II), which is evidenced by the ~513 Ma thick lower crust-derived adakitic rocks, such as the Datongdong and Yirba plutons (e.g. Liu et al., 2014; Yin et al., 2020). Subsequently, West Kunlun crust had thickened from 37.7 km (480 Ma) to 63.3 km (460 Ma) (Cycle III). Zircons extracted from the Akedala pluton also provide a positive test to crustal thickening in Cycle III. The thick lower crust-derived adakitic nature for the 470–452 Ma Datong (most of the samples) and Akedala plutons (Li et al., 2019; Liao et al., 2010; Wang et al., 2017; Xu et al., 2021; Zhu et al., 2018) lends additionally petrological supports for the Cycle III thickening event. West Kunlun crust abruptly gained a thickness >70 km (430 Ma) and lost its thickness at Early Devonian (Cycle IV). Ca. 430 Ma thick lower crust-derived adakitic rocks (e.g. most of Buya samples; Hu, Guo, et al., 2017; Ye et al., 2008) and 405 Ma A-type rocks (e.g. North Kudi pluton; Xiao et al., 2005; Yuan et al., 2002) confirm the observed crustal thickness variations for Cycle IV.

## 4.2 | Proto-Tethyan orogenic processes

It is well recognized that Tarim Block (including NKT) collided with SKT-TSHT at early Silurian (e.g. Zhang, Zou, et al., 2019). The collisional event is marked by the ~440 Ma amphibolite-facies metamorphism in SKT (Zhang, Zou, et al., 2019). Adakitic magmatism during Cycle IV thickening event (450–400 Ma) was mainly thick lower crust-derived and generated rocks that share comparably elevated La/Yb ratios (Figure 3) with those of 35–9 Ma adakites during the tectonic thickening of Tibetan Plateau (Zhu et al., 2017). Proto-Tethyan crustal thickening during Cycle IV can be primarily attributed to tectonic thickening due to underplating of the subducted, buoyant Tarim continental lithosphere and intracontinental thrusting. A-type felsic magmatism occurred when tectonic transition prevailed. Devonian red molasse formation (Zhang, Zou, et al., 2019) records post-collisional orogenic collapse.

We propose that the Proto-Tethyan West Kunlun has undergone previously-unrecognized accretionary orogenic processes prior to the 440 Ma continent-continent collision. Supporting evidences are as follows: (1) Proto-Tethyan southward subduction generated an Early Palaeozoic magmatic belt dominated by intermediate to felsic rocks with minor mafic rocks in West Kunlun (Figure 2b), consistent with the scenario of the Cordilleran orogenic belt in North America (DeCelles et al., 2009); (2) remarkable thickened crust (over 60 km) was attained at ~513 and ~460 Ma before the occurrence of collision-related amphibolite-facies metamorphism (Figure 4); (3) episodic crustal thickening and thinning processes in West Kunlun display a similar 40 Myr cyclicity to the Cordilleran orogenic systems in the Coast Mountains and Sierra Nevada (DeCelles et al., 2009;

Profeta et al., 2015); (4) the Ediacaran to Ordovician Saitula Group in SKT was recently proposed to be a large accretionary wedge added to the northern margin of TSHT (Zhang, Zou, et al., 2019). Reconstructed crustal thickness variations over time demonstrate two episodes of accretionary orogeneses at Cycle II (520–480 Ma) and Cycle III (480–450 Ma), respectively. Proto-Tethyan accretionary orogeneses together with the succeeding collisional orogenesis fit the prediction of the Wilson cycle.

Repeated crustal shortening and high-flux magmatism injection provide well explanations for the episodically crustal thickening of the Cordilleran accretionary orogenic systems (DeCelles et al., 2009). The main contribution from crustal shortening to the Cycle II and Cycle III accretionary orogeneses in West Kunlun cannot be confirmed because no coeval structural geology evidence has been reported at the duration. Nonetheless, high-flux magmatism injection events should have exerted a significant influence on crustal thickening during Cycle II and Cycle III. Profound pulses of high-flux magmatism at 511 and 458 Ma were recovered by detrital zircons and are in good agreement with the timing of thickening events (Figure 5a). The shifts in zircon Hf isotopic compositions toward negative values at 510 and 470–450 Ma magmatic flare-ups reflect progressively more input of compositionally evolved materials (Figure 5b), which is a common feature for high-flux episodes in Cordilleran accretionary orogenic belts (DeCelles et al., 2009).

### 4.3 | Proto-Tethyan and Gondwanan geodynamic affinity

Along the eastern margin of Gondwana, there are two successively younger outboard, Early Palaeozoic orogens (Figure 1), including the Delamerian Orogen (500–490 Ma) and the Lachlan Orogen (440–400 Ma; e.g. Collins et al., 2019). These orogens were regarded as a long-lived retreating accretionary orogenic system because no collider has been identified. Oceanic asperities (e.g. oceanic plateaus and ridges) have thereby been proposed to periodically, albeit transiently, chocked but eventually pass through the subduction zone to account for these successive orogenic contractional events (Collins et al., 2019).

However, the recognition of coeval Early Palaeozoic orogeneses in the northern margin of Gondwana in this study casts doubt on the validity of "oceanic asperities" in the opposite side of the supercontinent. Here, we show that Cycle II accretionary orogenesis (520–480 Ma) and Cycle IV collisional orogenesis (450–400 Ma) in

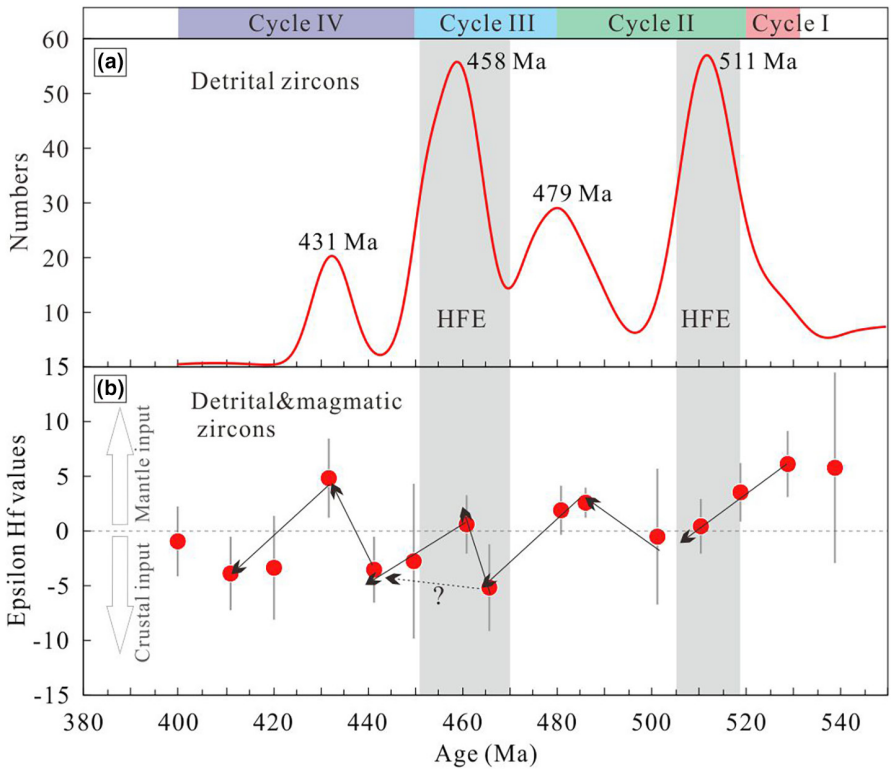


FIGURE 5 U-Pb age spectrum for Early Palaeozoic detrital zircons (a) and variations of epsilon Hf values for Early Palaeozoic detrital and magmatic zircons (b) in West Kunlun. Detrital zircons reveal two major high-flux episodes (HFEs) at 511 and 458 Ma and two subordinate episodes at 479 and 431 Ma. Note the two major HFEs coincide with the crustal thickening events during Cycle II and Cycle III, respectively. The two major HFEs also correspond to overall negative shifts of epsilon Hf values, indicating significantly increasing inputs of evolved continental components during Cycle II and Cycle III crustal thickening processes. By contrast, the two subordinate episodes at 479 and 431 Ma record more inputs of the depleted mantle, likely reflecting slab window or slab breakoff events. Slab window or slab breakoff events may also occur during Cycle III as evidenced by the positive shift of epsilon Hf values at 460 Ma and the presence of coeval oceanic crust-derived adakitic rocks (some Datong samples). The data are from Zhu et al. (2021) and references therein. [Colour figure can be viewed at wileyonlinelibrary.com]

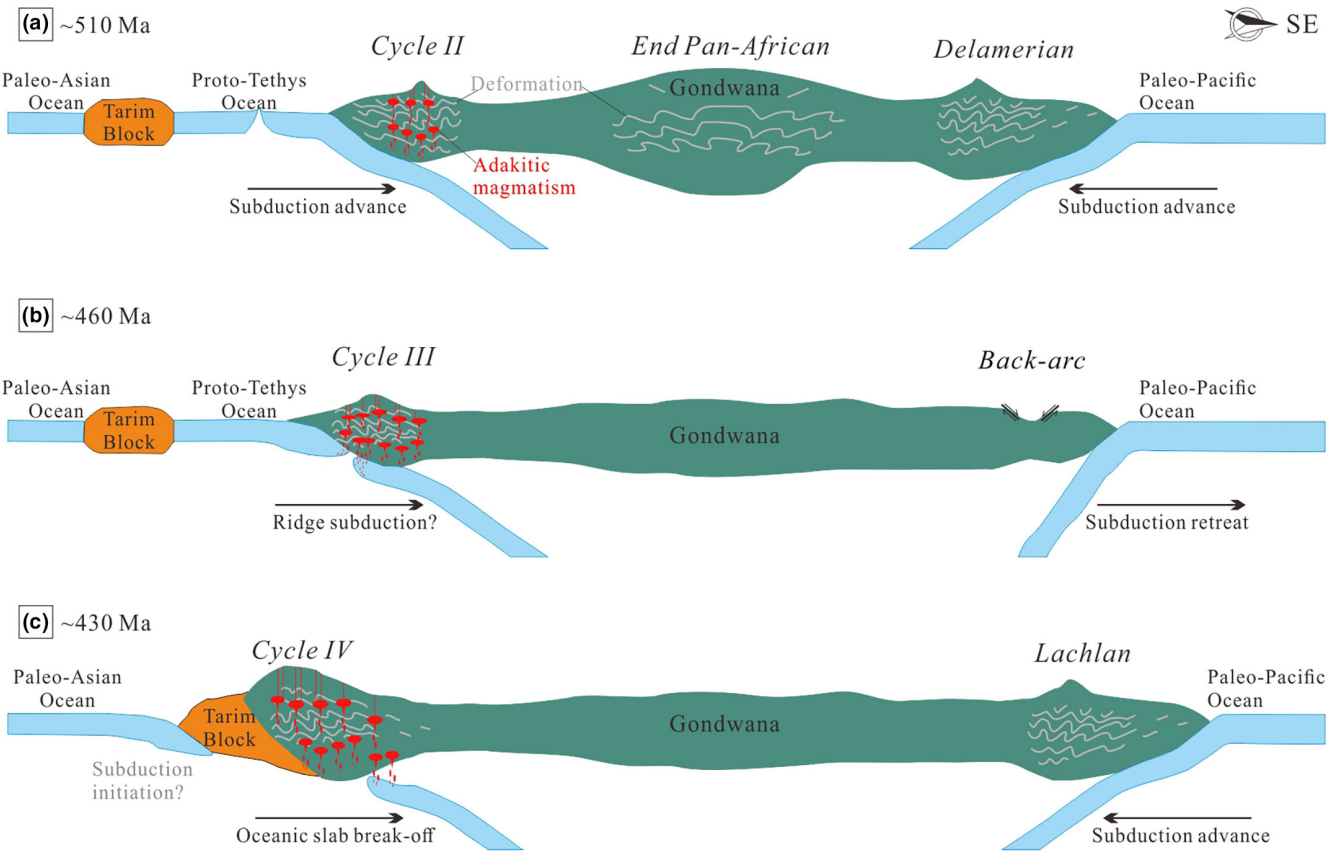


**FIGURE 6** Schematic model showing the coeval Early Palaeozoic orogeneses along the northern and eastern margins of Gondwana. The profile comes from the dashed line (a and b) in Figure 1. Also shown is the end of the Pan-African orogens (~520–500 Ma; Cawood & Buchan, 2007). [Colour figure can be viewed at wileyonlinelibrary.com]

Proto-Tethyan West Kunlun highly coincided with the Delamerian (520–490 Ma) and the Lachlan (440–400 Ma) accretionary contractional orogeneses, respectively (Figure 6). Such a coincidence cannot be simply attributed to the episodic subduction of oceanic plateaus and ridges. Where oceanic plateaus exist and when oceanic plateaus/ridges will enter the subduction zones are rather random events during the Wilson cycles of two different oceanic basins (Proto-Tethyan vs. Paleo-Pacific). Alternatively, synchronous orogeneses could share similarly geodynamic mechanisms. Here, we propose accretionary orogenesis could be caused by continent-continent collision across the continent distance like the scenario of induced subduction initiation (Stern & Gerya, 2018). To be specific, the end Pan-African orogeny (520–500 Ma; Cawood & Buchan, 2007) within the Gondwana generated the coeval compression along the northern and eastern margins of the supercontinent (Figure 6a). In turn, the collision between Greater South China-North China-Alax-Dunhuang-Tarim blocks and northern Gondwana triggered the 450–400 Ma Lachlan orogenesis in the opposite side of the supercontinent (Figure 6c).

Admittedly, Cycle III accretionary orogenesis (480–450 Ma) in West Kunlun could be a rather local event. Co-existence of subducted oceanic crust- and thick lower crust-derived adakites (e.g. Datong pluton; Li et al., 2019; Liao et al., 2010; Wang et al., 2017; Zhu et al., 2018) together with a sharp shift in zircon Hf isotopic compositions toward positive values at 460 Ma are somewhat consistent with the subduction of oceanic ridges or slab breakoff, which deserves further study.

## 5 | IMPLICATIONS

Significant accretionary orogeneses at 520–450 Ma were identified before the 450–400 Ma collisional orogenesis in Proto-Tethyan West Kunlun. In West Kunlun, 520–480 Ma accretionary orogenesis was a geodynamical response to the final collision among blocks within Gondwana. In turn, 450–400 Ma collision between Tarim and northern margin of Gondwana triggered the Lachlan accretionary orogenesis along the opposite margin. The Wilson cycle of an ocean ends up with compensatory enhancement of convergence in neighbouring tectonic domains.

### ACKNOWLEDGEMENTS

This study received financial support from the National Natural Science Foundation of China (Grants U1603245 and 42002210) and the Open Project Fund of the State Key Laboratory of Ore Deposit Geochemistry, Institute of Geochemistry, Chinese

Academy of Sciences (202212). Insightful comments from the editor and three anonymous reviewers helped clarify the idea expressed here.

## DATA AVAILABILITY STATEMENT

The data that support the findings of this study are available from the corresponding author upon reasonable request.

## REFERENCES


Cawood, P. A. (2005). Terra Australis Orogen: Rodinia breakup and development of the Pacific and Iapetus margins of Gondwana during the Neoproterozoic and Paleozoic. *Earth-Science Reviews*, *69*, 249–279. https://doi.org/10.1016/j.earscirev.2004.09.001

Cawood, P. A., & Buchan, C. (2007). Linking accretionary orogenesis with supercontinent assembly. *Earth-Science Reviews*, *82*, 217–256. https://doi.org/10.1016/j.earscirev.2007.03.003

Cawood, P. A., Kröner, A., Collins, W. J., Kusky, T. M., Mooney, W. D., & Windley, B. F. (2009). Accretionary orogens through Earth history. In P. A. Cawood & A. Kröner (Eds.), *Earth accretionary systems in space and time* (Vol. *318*, pp. 1–36). Geological Society, Special Publications. https://doi.org/10.1144/SP318.1

Collins, W. J., Huang, H. Q., Bowden, P., & Kemp, A. I. S. (2019). Repeated S–I–A-type granite trilogy in the Lachlan Orogen and geochemical contrasts with A-type granites in Nigeria: implications for petrogenesis and tectonic discrimination. *Geological Society, London, Special Publications*, *491*, 53–76. https://doi.org/10.1144/SP491-2018-159

Cui, J. T., Wang, J. C., Bian, X. W., Luo, Q. Z., Zhu, H. P., Wang, M. C., & Chen, G. C. (2007). Zircon SHRIMP U-Pb dating of the Dongbake gneissic tonalite in northern Kangxiwar, West Kunlun. *Geological Bulletin of China*, *26*, 726–729. https://doi.org/10.1016/S1872-5791(07)60044-X

Cui, J. T., Wang, J. C., Bian, X. W., Zhu, H. P., Luo, Q. Z., Yang, K. J., & Wang, M. C. (2007). Zircon SHRIMP U-Pb dating of early Paleozoic granite in the Menggubao-Pushou area on the northern side of Kangxiwar, West Kunlun. *Geological Bulletin of China*, *26*, 710–719. in Chinese with English abstract. https://doi.org/10.3969/j.1671-2552.2007.06.012

Cui, J. T., Wang, J. C., Bian, X. W., Zhu, H. P., & Yang, K. J. (2006). Geological characteristics of early Paleozoic amphibolite and tonalite in northern Kangxiwar, West Kunlun, China and their zircon SHRIMP U-Pb dating. *Geological Bulletin of China*, *25*, 1441–1449 in Chinese with English abstract.

DeCelles, P. G., Ducea, M. N., Kapp, P., & Zandt, G. (2009). Cyclicity in Cordilleran orogenic systems. *Nature Geoscience*, *2*, 251–257. https://doi.org/10.1038/ngeo469

Gao, X. F., Xiao, P. X., Kang, L., Zhu, H. P., Guo, L., Xi, R. G., & Dong, Z. C. (2013). Origin of the volcanic rocks from the Ta' axi region, Taxkorgan Xinjiang and its geological significance. *Earth Science-Journal of China University of Geosciences*, *38*, 1769–1182 in Chinese with English abstract.

He, B. Z., Jiao, C. L., Xu, Z. Q., Cai, Z. H., Zhang, J. X., Liu, S. L., Li, H. B., Chen, W. W., & Yu, Z. Y. (2016). The paleotectonic and paleogeography reconstructions of the Tarim Basin and its adjacent areas (NW China) during the late Early and Middle Paleozoic. *Gondwana Research*, *30*, 191–206. https://doi.org/10.1016/j.gr.2015.09.011

He, R. Z., Liu, G. C., Golos, E., Gao, R., & Zheng, H. W. (2014). Isostatic gravity anomaly, lithospheric scale density structure of the northern Tibetan plateau and geodynamic causes for potassic lava eruption in Neogene. *Tectonophysics*, *628*, 218–227. https://doi.org/10.1016/j.tecto.2014.04.047

Hu, J., Wang, H., Huang, C., Tong, L., Mu, S., & Qiu, Z. (2016). Geological characteristics and age of the dahongliutan fe-ore deposit in the western kunlun orogenic belt, Xinjiang, northwestern China. *Journal of Asian Earth Sciences*, *116*, 1–25. https://doi.org/10.1016/j.jseaes.2015.08.014

Hu, J., Wang, H., Mu, S. L., Wang, M., & Hou, X. W. (2017). Geochemistry and Hf isotopic compositions of early Paleozoic granites in Nanpingxueshan from the Tianshuihai terrane, west Kunlun: Crust-mantle magmatism. *Acta Geologica Sinica*, *91*, 1192–1207 in Chinese with English abstract.

Hu, X. Y. (2018). *Petrogenesis and tectonic significance of granitic pluton and MMEs in the eastern segment of the Tiekelike* (pp. 1–69). Xinjiang University. Master thesis. In Chinese with English abstract.

Hu, X. Y., Guo, R. Q., Nuer, K. M., Guo, Y., Zhou, M. Y., & Lv, B. (2017). Zircon U-Pb dating, petrology, geochemistry of the buya pluton and its mmes in the southern margin of tarim. *Rock and Mineral Analysis*, *36*, 538–550 In Chinese with English abstract.

Jia, R. Y., Jiang, Y. H., Liu, Z., Zhao, P., & Zhou, Q. (2013). Petrogenesis and tectonic implications of early Silurian high-K calc-alkaline granites and their potassic microgranular enclaves, western Kunlun orogen, NW Tibetan plateau. *International Geology Review*, *55*, 958–975. https://doi.org/10.1080/00206814.2012.755766.8

Li, S. Z., Yang, Z., Zhao, S. J., Liu, X., Yu, S., Li, X. Y., Guo, L. L., Suo, Y. H., Dai, L. M., Guo, R. H., & Zhang, G. W. (2016). Global early paleozoic orogens (IV), plate reconstruction and supercontinent Carolina. *Journal of Jilin University (Earth Science Edition)*, *46*(4), 1026–1041 (in Chinese with English abstract).

Li, S. Z., Zhao, S. J., Liu, X., Cao, H., Yu, S., Li, X. Y., Somerville, I., & Yu, S. Y. (2018). Closure of the proto-Tethys Ocean and Early Paleozoic amalgamation of microcontinental blocks in East Asia. *Earth-Science Reviews*, *186*, 37–75. https://doi.org/10.1016/j.earscirev.2017.01.011

Li, Y., Xiao, W., & Tian, Z. (2019). Early Palaeozoic accretionary tectonics of west kunlun orogen: Insights from Datong granitoids, mafic–ultramafic complexes, and silurian-devonian sandstones, Xinjiang, NW China. *Geological Journal*, *54*, 1505–1517. https://doi.org/10.1002/gj.3246.3

Liao, S. Y., Jiang, Y. H., Jiang, S. Y., Yang, W. Z., Zhou, Q., Jin, G. D., & Zhao, P. (2010). Subducting sediment-derived arc granitoids: Evidence from the Datong pluton and its quenched enclaves in the western Kunlun orogen, Northwest China. *Mineralogy and Petrology*, *100*, 55–74. https://doi.org/10.1007/s00710-010-0122-x

Liu, X., Zhu, Z. X., Guo, R. Q., Zhu, Y. F., Li, P., & Jin, L. Y. (2016). LAICP-MS zircon U-Pb dating and its geological significance for Late Paleozoic diabase from the west part of Tiekelike area, South Tarim. *Geological Sciences*, *3*, 794–805. in Chinese with English abstract. https://doi.org/10.12017/dzkx.2016.030

Liu, X. Q., Zhang, C. L., Ye, X. T., Zou, H., & Hao, X. S. (2019). Cambrian mafic and granitic intrusions in the Mazar-Tianshuihai terrane, west kunlun orogenic belt: Constraints on the subduction orientation of the proto-tethys ocean. *Lithos*, *350*, 105226. https://doi.org/10.1016/j.lithos.2019.105226

Liu, Z., Jiang, Y. H., Jia, R. Y., Zhao, P., Zhou, Q., Wang, G. C., & Ni, C. Y. (2014). Origin of middle Cambrian and Late Silurian potassic granitoids from the western Kunlun orogen, Northwest China: A magmatic response to the proto-Tethys evolution. *Mineralogy and Petrology*, *108*, 91–110. https://doi.org/10.1007/s00710-013-0288-0.1

Matte, P., Tapponnier, P., Arnaud, N., Bourjot, L., Avouac, J. P., Vidal, P., Liu, Q., Pan, Y. S., & Wang, Y. (1996). Tectonics of Western Tibet, between the Tarim and the Indus. *Earth and Planetary Science Letters*, *142*, 311–330. https://doi.org/10.1016/0012-821X(96)00086-6

Profeta, L., Ducea, M. N., Chapman, J. B., Paterson, S. R., Gonzales, S. M. H., Kirsch, M., Petrescu, L., & DeCelles, P. G. (2015). Quantifying crustal thickness over time in magmatic arcs. *Scientific Reports*, *5*, 1–7. https://doi.org/10.1038/srep17786

Rowley, D. B. (2013). Sea level: Earth's dominant elevation—Implications for duration and magnitudes of sea level variations. *The Journal of Geology*, *121*, 445–454. https://doi.org/10.1086/671392

Rudnick, R. L., & Gao, S. (2003). Composition of the continental crust. *Treatise on Geochemistry*, *3*, 1–64. https://doi.org/10.1016/B978-0-08-095975-7.00301-6ù

Stern, R. J., & Gerya, T. (2018). Subduction initiation in nature and models: A review. *Tectonophysics*, *746*, 173–198. https://doi.org/10.1016/j.tecto.2017.10.014

Tang, G. J., Wang, Q., Wyman, D. A., Li, Z. X., Zhao, Z. H., Jia, X. H., & Jiang, Z. Q. (2010). Ridge subduction and crustal growth in the Central Asian Orogenic Belt: Evidence from Late Carboniferous adakites and high-Mg diorites in the western Junggar region, northern Xinjiang (West China). *Chemical Geology*, *277*, 281–300. https://doi.org/10.1016/j.chemgeo.2010.08.012

Tang, M., Chu, X., Hao, J. H., & Shen, B. (2021). Orogenic quiescence in Earth's middle age. *Science*, *371*(6530), 728–731. https://doi.org/10.1126/science.abf1876

Tang, M., Ji, W. Q., Chu, X., Wu, A. B., & Chen, C. (2020). Reconstructing crustal thickness evolution from europium anomalies in detrital zircons. *Geology*, *49*, 76–80. https://doi.org/10.1130/G47745.1

Wang, C., Liu, L., He, S. P., Yang, W. Q., Cao, Y. T., & Zhu, X. H. (2013). Early Paleozoic magmatism in west Kunlun: Constrains from geochemical and zircon U-Pb-Hf isotope studies of the Bulong granite. Chinese. *Journal of Geology*, *48*, 997–1014 In Chinese with English abstract.

Wang, J., Hattori, K., Liu, J., Song, Y., Gao, Y., & Zhang, H. (2017). Shoshonitic-and adakitic magmatism of the early Paleozoic age in the western kunlun orogenic belt, nw China: Implications for the early evolution of the northwestern Tibetan plateau. *Lithos*, *286*, 345–362. https://doi.org/10.1016/j.lithos.2017.06.013

Xiao, W. J., Windley, B. F., Liu, D. Y., Jian, P., Liu, C. Z., Yuan, C., & Sun, M. (2005). Accretionary tectonics of the western Kunlun orogen, China: A Paleozoic-early Mesozoic, long lived active continental margin with implications for the growth of southern Eurasia. *The Journal of Geology*, *113*, 687–705. https://doi.org/10.1086/449326.6

Xiao, X. C., Wang, J., Su, L., & Song, S. G. (2003). A further discussion of the Küda ophiolite, West Kunlun, and its tectonic significance. *Geological Bulletin of China*, *22*, 645–750 (in Chinese with English abstract).

Xu, J. H., Zhang, Z. W., Wu, C. Q., Li, X. Y., Jin, Z. R., Hu, P. C., Luo, T. Y., & Zhu, W. G. (2021). Petrogenesis and tectonic implications of Early Paleozoic granitoids in the Qiaerlong district of the West Kunlun orogenic belt: Constraints from petrology, geochronology, and Sr-Nd-Hf isotope geochemistry. *International Geology Review*, *2021*, 1882888. https://doi.org/10.1080/00206814.2021.1882888

Ye, H. M., Li, X. H., Li, Z. X., & Zhang, C. L. (2008). Age and origin of high Ba–Sr appinite–granites at the northwestern margin of the Tibet Plateau: Implications for early Paleozoic tectonic evolution of the Western Kunlun orogenic belt. *Gondwana Research*, *13*, 126–138. https://doi.org/10.1016/j.gr.2007.08.005.1

Yin, A., & Harrison, T. M. (2000). Geologic evolution of the Himalayan–Tibetan orogen. *Annual Review of Earth and Planetary Sciences*, *28*, 211–280. https://doi.org/10.1146/annurev.earth.28.1.211

Yin, J., Xiao, W., Sun, M., Chen, W., Yuan, C., Zhang, Y., & Xia, X. (2020). Petrogenesis of early Cambrian granitoids in the western Kunlun orogenic belt, Northwest Tibet: Insight into early stage subduction of the Proto-Tethys Ocean. *Geological Society of America Bulletin*, *132*, 2221–2240. https://doi.org/10.1130/B35408.1

Yuan, C., Sun, M., Zhou, M. F., Xiao, W. J., & Zhou, H. (2005). Geochemistry and petrogenesis of the Yishak Volcanic sequence, Kudi ophiolite, West Kunlun (NW China): Implications for the magmatic evolution in a subduction zone environment. *Contributions to Mineralogy and Petrology*, *150*, 195–211. https://doi.org/10.1007/s00410-005-0012-0

Yuan, C., Sun, M., Zhou, M. F., Zhou, H., Xiao, W. J., & Li, J. L. (2002). Tectonic evolution of the West Kunlun: Geochronologic and geochemical constraints from Kudi Granitoids. *International Geology Review*, *44*, 653–669. https://doi.org/10.2747/0020-6814.44.7.653.7

Zhang, C. L., Zou, H. B., Ye, X. T., & Chen, X. Y. (2018a). Timing of subduction initiation in the Proto-Tethys Ocean: Evidence from the Cambrian gabbros from the NE Pamir plateau. *Lithos*, *314*, 40–51. https://doi.org/10.1016/j.lithos.2018.05.021.4

Zhang, C. L., Zou, H. B., Ye, X. T., & Chen, X. Y. (2018b). Tectonic evolution of the NE section of the Pamir Plateau: New evidence from field observations and zircon U-Pb geochronology. *Tectonophysics*, *723*, 27–40. https://doi.org/10.1016/j.tecto.2017.11.036

Zhang, C. L., Zou, H. B., Ye, X. T., & Chen, X. Y. (2019). Tectonic evolution of the West Kunlun Orogenic Belt along the northern margin of the Tibetan Plateau: Implications for the assembly of the Tarim terrane to Gondwana. *Geoscience Frontiers*, *10*, 973–988. https://doi.org/10.1016/j.gsf.2018.05.006.3

Zhang, H. S., He, S. P., Ji, W. H., Wang, C., Shi, J. B., Kang, K. Y., & Xi, D. H. (2016). Implications of late cambrian granite in tianshuihai massif for the evolution of proto tethy ocean: Evidences from zircon geochronology and geochemistry. *Acta Geologica Sinica*, *90*, 2582–2602 in Chinese with English abstract.

Zhang, J. X., Yu, S. Y., & Mattinson, C. G. (2017). Early Paleozoic polyphase metamorphism in northern Tibet, China. *Gondwana Research*, *41*, 267–289. https://doi.org/10.1016/j.gr.2015.11.009

Zhang, Q., Liu, Y., Huang, H., Wu, Z., & Zhou, Q. (2016). Petrogenesis and tectonic implications of the high-K Alamas calc-alkaline granitoids at the northwestern margin of the Tibetan plateau: Geochemical and Sr-Nd-Hf-O isotope constraints. *Journal of Asian Earth Sciences*, *127*, 137–151. https://doi.org/10.1016/j.jseaes.2016.05.026

Zhang, Q., Wu, Z., Chen, X., Zhou, Q., & Shen, N. (2019). Proto-Tethys oceanic slab break-off: Insights from early Paleozoic magmatic diversity in the West Kunlun Orogen. *NW Tibetan Plateau. Lithos*, *346*, 105147. https://doi.org/10.1016/j.lithos.2019.07.014

Zhang, Q., Wu, Z. H., Li, S., Li, K., Liu, Z. W., & Zhou, Q. (2019). Ordovician granitoids and silurian mafic dikes in the western kunlun orogen, Northwest China: Implications for evolution of the proto-tethys. *Acta Geologica Sinica-english Edition*, *93*, 30–49. https://doi.org/10.1111/1755-6724.13760.1

Zhang, Y. G., Yao, X. Z., Wang, J., Pan, W. Q., Chen, Y. Q., Zhang, B. S., & Yang, T. (2022). U-Pb ages and europium anomalies of detrital zircons from sediments in the West Kunlun Orogenic Belt: Implications for the Proto-Tethys Ocean evolution. *Journal of Earth Science*. https://doi.org/10.1007/s12583-022-1671-8

Zhang, Z. W., Cui, J. T., Wang, J. C., Bian, X. W., Zhu, H. P., Luo, Q. Z., & Wang, M. C. (2007). SHRIMP U-Pb dating of early Paleozoic amphibolite and granodiorite in Korliang, northwestern Kangxiwa, West Kunlun. *Geological Bulletin*, *26*, 720–725 in Chinese with English abstract.

Zheng, Y. Z., Yang, W. W., & Wang, T. (2013). Geochemistry and geological significance of intrusive rocks of early Paleozoic in Western Kunlun, Xinjiang. *Northwestern Geology*, *4*, 57–65. in Chinese with English abstract. https://doi.org/10.3969/j.1009-6248.2013.04.006

Zhou, H., Chu, Z. Y., Li, J. L., Hou, Q. L., Wang, Z. H., & Fang, A. M. (2000). $^{40}Ar/^{39}Ar$ dating of ductile shear zone in Kuda, west Kunlun, Xinjiang. *Scientia Geologica Sinica*, *35*, 233–239 in Chinese with English abstract.

Zhu, D. C., Wang, Q., Cawood, P. A., Zhao, Z. D., & Mo, X. X. (2017). Raising the Gangdese Mountains in southern Tibet. *Journal of Geophysical Research: Solid Earth*, *122*, 214–223. https://doi.org/10.1002/2016JB013508

Zhu, G. Y., Liu, W., Wu, G. H., Ma, B. S., Nance, R. D., Wang, Z. C., Xiao, Y., & Chen, Z. Y. (2021). Geochemistry and U-Pb-Hf detrital zircon geochronology of metamorphic rocks in terranes of the West Kunlun Orogen: Protracted subduction in the northernmost proto-Tethys Ocean. *Precambrian Research*, *363*, 106344. https://doi.org/10.1016/j.precamres.2021.106344

Zhu, J., Li, Q., Chen, X., Tang, H., Wang, Z., Chen, Y., & Chen, J. (2018). Geochemistry and petrogenesis of the early Palaeozoic appinite-granite complex in the western Kunlun orogenic belt, NW China: Implications for Palaeozoic tectonic evolution. *Geological Magazine*, *155*, 1641–1666. https://doi.org/10.1017/S0016756817000450.8

Zhu, J., Li, Q. G., Wang, Z. Q., Tang, H. S., Chen, X., & Xiao, B. (2016). Magmatism and tectonic implication of early Cambrian granitoid plutons in Tianshuhai Terrane of the western kunlun orogenic belt, Northwest China. Northwestern. *Geology*, *49*, 1–18 In Chinese with English abstract.

Zhuan, S. P., Bai, C. D., Mao, Z. F., Li, D., Zhang, X. Z., Chen, Y. Y., & Lian, Q. (2018). Zircon U-Pb ages and geochemical characteristics of the Sugaitilike late Silurian granites in southern Kudi, Xinjiang and its geotectonic significance. *Journal of Geomechanics*, *24*, 661–669. https://doi.org/10.12090/j.issn.1006-6616.2018.24.05.066 in Chinese with English abstract.

## SUPPORTING INFORMATION

Additional supporting information can be found online in the Supporting Information section at the end of this article.

**FIGURE S1.** Chondrite-normalized REE diagrams for magmatic zircons from the Akedala pluton. Normalization data of chondrite are from Sun & McDonough (1989).

**FIGURE S2.** Diagrams of zircon P content vs. zircon La content (a), zircon Eu/Eu* (b) and zircon U-Pb age (c). U-Pb ages with two sigma errors are shown in c. U-Pb ages come from Xu et al. (2021).

**FIGURE S3.** Diagrams of $SiO_2$ vs. $Na_2O+K_2O$ (a), $SiO_2$ vs. MgO (b), $SiO_2$ vs. $K_2O$ (c) and A/CNK vs. A/NK (d) for complied Early Palaeozoic magmatic rocks before filtering. Data sources of Early Palaeozoic magmatic rocks as Figure 2. Reference fields in b are from Tang et al. (2010) and references therein.

**TABLE S1.** LA-ICP-MS zircon trace element analyses for the Akedala pluton in the West Kunlun orogenic belt, northwest China

**TABLE S2.** A summary of Early Palaeozoic magmatism in the West Kunlun orogenic belt

**How to cite this article:** Wang, Y.-J., Zhu, W.-G., Zhang, Z.-W., Yang, K., Wu, C.-Q., Xu, J.-H., Leng, C.-B., & Xu, J.-B. (2023). Accretionary orogenesis triggered by collision across continent distance: Evidence from the Proto-Tethyan West Kunlun, China. *Terra Nova*, *35*, 193–202. https://doi.org/10.1111/ter.12643